Assessment of a Dual-Wavelength Compensation Technique for Displacement Sensors Using Plastic Optical Fibers

Alberto Vallan, *Member, IEEE*, Maria Luisa Casalicchio, Massimo Olivero and Guido Perrone *Member, IEEE*

***Abstract*—The paper analyzes the performance of a dual-wavelength technique devised to compensate power fluctuations in intensity-modulated plastic optical fiber sensors, which were specifically conceived for the measurement of displacements in industrial and civil applications. These sensors retrieve the displacement from the variation of the attenuation along the light path and use two signals at different wavelengths to compensate for the effects of parasitic quantities, such as temperature and strains along the fiber. The theoretical behavior of the compensation technique is presented and the results of experiments carried out with different combinations of signal wavelengths and plastic fibers are reported. The experimental setup has proved that, by proper choice of the compensation signal wavelength, it is possible to monitor displacements in the range (0 to 10) mm, even for low received power and under severe perturbation conditions, thus significantly improving the long-term stability of the sensors.**

***Index Terms*—Optical Fibers, Plastic Optical Fibers (POF), Optical Fiber Sensors, Displacement Measurement.**

A. Vallan, M.L. Casalicchio, M. Olivero, and G. Perrone are with the Dipartimento di Elettronica, Politecnico di Torino, corso Duca degli Abruzzi, 24 - 10129 Torino (Italy); phone: +39 011 0904110, fax: +39 011 0904217, e–mail: alberto.vallan@polito.it This work has been supported by Piemonte local government within the project Laserfactory (Bando Sistemi di produzione 2008).

I. Introduction

Fiber Optic Sensors (FOS) are finding increasing use in structural health monitoring [1] and in industrial applications [2] because of their well known advantages, such as immunity to electromagnetic interferences, minimum invasive impact, intrinsic fire safety, possibility of being embedded into the material, etc.

Different working principles have been exploited to relate one of the characteristic of light propagating along a fiber (intensity, phase, frequency, polarization) with the quantity under measurement. Among these, intensity-modulated sensors (also known as intensiometric sensors) represent the most straightforward and basic type of FOS [3]-[4], since intensity variations are the easiest to measure.

In the past, fiber sensors were considered a sort of secondary market for devices originally developed for the telecommunication industry and therefore they were made only with single- or multi-mode silica fibers with small core (tens to hundreds of micrometers) and low numerical aperture (0.1 to 0.3). However, in the last years several research groups have pioneered the development of sensors based on Plastic Optical Fibers (POF), a

type of fiber characterized by quite large core (typically 0.25 mm to 1 mm) and high numerical aperture (≈ 0.5). With these characteristics, POF are particularly suitable for the realization of intensiometric displacement sensors because they enable a tenfold increase of the measurement range with respect to their glass fiber based equivalents, reaching up to tens of millimeters. Moreover, a large core diameter also represents a benefit in terms of roughness, dust tolerance, and ease of installation.

Relying on POF technology, the authors have already developed a low-cost monitoring system using intensity-modulated sensors to monitor mechanical quantities, such as vibrations and displacements, for industrial [5] and structural [6] applications.

The main drawback of intensity-modulated sensors, however, is their large sensitivity to external perturbations (e.g. temperature, micro-bending and mechanical stress in general), which result in variation of the received signal indistinguishable from that produced by actual modification of the displacement. A certain number of schemes have been studied to compensate these power fluctuations in POF sensors [7], including the usage of dummy sensors [8], whose displacement readings depend on environmental stimuli (temperature, humidity) only. In particular, the dummy sensor technique helps in lowering the sensitivity to temperature down to acceptable values, but it cannot correct uncertainties due to mechanical stress along the fiber since these effects are typically dependent on the specific fiber span [9]. However, as shown in [9], higher stability sensors can be realized by slightly modifying the fiber tip of a conventional reflection-based intensiometric displacement sensor, introducing a wavelength-selective element and feeding the system with two signals at different wavelengths, one used to measure the displacement and the other to correct the sensor reading for environmental disturbances.

This dual wavelength approach as a compensation technique for intensity-based optical fiber sensors was presented in a comprehensive paper by G. Murtaza et al. in 1995 [10], though former studies date back to 1984. In [10] the authors analyzed a number of sensor configurations exploiting the dual wavelength technique, focusing on the thermal behavior of the sources and relying on lab-arranged setup. In [9] we demonstrated the feasibility of this dual wavelength compensation technique with POF-based intensiometric sensors; however, to the best of our knowledge, a turnkey sensing system relying on POF sensors with this type of compensation technique has never been investigated to assess its behavior in realistic working conditions.

In this paper, after a summary of the classical intensiometric displacement sensor working principle and of the effects occurring in long-term measurements, we describe the proposed compensation technique from a theoretical point of view to evaluate the sensor expected performance; then, we report on the experimental assessments carried out with different combinations of wavelengths and types of plastic fibers under realistic operating conditions.

II. The sensor working principle and long-term issues

The basic sensor architecture, shown in Fig. 1, is made of an optical source OS, a couple of plastic optical fibers, a reflecting surface (a mirror in Fig. 1) acting a movable target, and an optical detector PD. The displacement is evaluated from the measurement of the signal coupled into one of the fibers after free-space forward and backward propagation over a distance d_{M} and reflection by the target. The detected optical power P_{r} thus depends on the launched optical power P, on

the optical sensor response $R(d_{\mathrm{M}})$, and on the loss A as:

$$P_{\mathrm{r}} = P \cdot A \cdot R(d_{\mathrm{M}}) \tag{1}$$

where $R(d_{\mathrm{M}})$ is a function of the target distance d_{M} and of the fiber geometrical and optical characteristics [5].

As discussed in [9], this sensor presents two working ranges separated by the response peak: in the leftmost region the sensitivity is highest but the usable working range is severely limited, and vice-versa for rightmost region. Sensors for monitoring small vibrations (like those often used in industrial applications) can exploit the first range, whereas for applications that require a larger working range (like in structural health monitoring) the sensor should be designed to operate in the rightmost region to have a good trade-off between range and sensitivity.

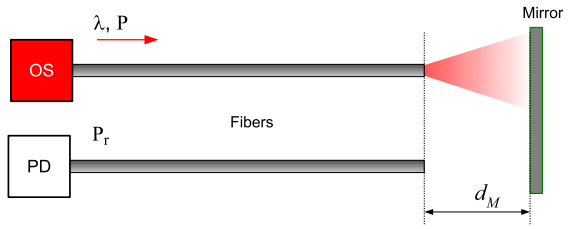

Fig. 1. The sensor structure: the optical source lights one of the fibers and the other fiber, coupled to a detector, collects the light reflected by a mirror.

The authors have arranged several sensors as in Fig. 1 in the last years. Some of them have been tested only in the laboratory using computer-controlled precision linear translation stages and climatic chambers to simulate the operating environment. Others have been used also in real in-situ cases to monitor the evolution of cracks in buildings in the framework of pilot projects devoted to cultural heritage preservation [8]. Moreover, in all the installations dummy sensors forced to have a null displacement have been added to test the stability over time. Therefore, a relevant amount of data has been collected over time, especially in the real cases, since for these applications measurements have been taken for very long periods (years) and compared also with traditional sensors (such as LVDT) placed nearby.

The obtained results highlighted that sensors as in Fig. 1 provide satisfactory metrological performance in the short term (days) only, since in that case the displacement can be measured with a standard uncertainty better than 10 μm; then their performance decreases in the medium and long term (months, years) because of optical power fluctuations related to unpredictable changes in fiber losses.

The authors have already faced the stability problem analyzing a compensation technique based on dummy sensors in previous works [6], [11]; moreover, they have also developed an hybrid solution that takes advantage of wireless sensor networks to reduce the fiber span still ensuring the intrinsically fire safety of the monitoring system [12]. However, all these techniques do not allow long fiber spans to be employed, thus limiting the possibility of using of this types of sensors in many long term monitoring applications.

The compensation technique whose performance are studied in this paper has been developed to overcome the problem of the POF loss stability in the long term, even for long fiber spans, aiming at the realization of an all-POF sensing system for permanent monitoring able to counteract the drifts due to fiber aging and to parasitic environmental effects.

III. Optical power effect reduction by means of a dual-wavelength compensation technique

The sensor structure, modified to implement the proposed compensation technique, is shown in Fig. 2.

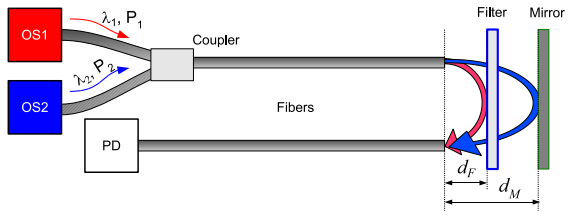

Fig. 2. The sensor structure modified to obtain compensation of fiber losses.

Two light emitting sources having wavelengths λ_1 and λ_2, respectively, are coupled to the transmitting fiber and are turned on and off alternately. An optical filter is placed between the fiber tips and the mirror. The filter position d_{F} is maintained constant with respect to the fiber tips. The filter is chosen to reflect the signal at λ_1 and to be transparent for the signal at λ_2.

The detected optical signals $P_{\mathrm{r}1}$ and $P_{\mathrm{r}2}$ when the sources OS1 and OS2 are active can be written as :

$$\begin{aligned} P_{\mathrm{r}1} &= P_1 \cdot A_1 \cdot R(d_{\mathrm{F}}) = k_1 \cdot R(d_{\mathrm{F}}) \\ P_{\mathrm{r}2} &= P_2 \cdot A_2 \cdot R(d_{\mathrm{M}}) = k_2 \cdot R(d_{\mathrm{M}}) \end{aligned} \tag{2}$$

where P_1 and P_2 are the source optical powers, A_1 and A_2 account for fiber and connectors attenuations at λ_1 and λ_2 respectively, and $R(d_{\mathrm{F}})$ and $R(d_{\mathrm{M}})$ are the sensor responses evaluated at the filter position d_{F} and at the mirror position d_{M}. It is well known that the attenuation of the plastic fibers is wavelength dependent [13], hence A_1 is different from A_2. As a first approximation, and for certain wavelengths, aging and temperature produce a wavelength-independent change of the fiber attenuation and, in case of constant optical powers P_1 and P_2, the ratio between the Eqn.s 2 becomes:

$$\frac{P_{\mathrm{r}2}}{P_{\mathrm{r}1}} = \frac{k}{R(d_{\mathrm{F}})} \cdot R(d_{\mathrm{M}}) \tag{3}$$

where $k/R(d_{\mathrm{F}})$ is constant. The result of Eqn. 3 shows that the sensor response is insensitive to changes in the fiber attenuation and in the power fluctuations, provided that their ratio is constant.

Real filters, like the one that will be described in the next section, are not able to completely reflect the signal at λ_1 and completely transmit the signal at λ_2. Therefore, indicating with T_1 and T_2 the filter transmission coefficients at λ_1 and λ_2, respectively, the detected optical powers can be rewritten as follow:

$$\begin{aligned} P_{\mathrm{r}1} &= P_1 \cdot A_1 \cdot \left[R(d_{\mathrm{F}}) \cdot (1 - T_1) + R(d_{\mathrm{M}}) \cdot T_1^2\right] \\ P_{\mathrm{r}2} &= P_2 \cdot A_2 \cdot \left[R(d_{\mathrm{F}}) \cdot (1 - T_2) + R(d_{\mathrm{M}}) \cdot T_2^2\right] \end{aligned} \tag{4}$$

The filter is chosen to have a small transmission coefficient T_1 at λ_1, typically below 1%; moreover, the sensor response at d_{M} is smaller than the response d_{F}. For these reasons the term $R(d_{\mathrm{M}})T_1^2$ can be neglected with respect to $R(d_{\mathrm{F}})(1 - T_1)$ and the power ratio becomes:

$$\begin{aligned} \frac{P_{\mathrm{r}2}}{P_{\mathrm{r}1}} &= k \cdot \left[\frac{1 - T_2}{1 - T_1} + \frac{T_2^2}{R(d_F(1 - T_1))} \cdot R(d_M)\right] = \\ &= k \cdot [a_0 + a_1 \cdot R(d_{\mathrm{M}})] \end{aligned} \tag{5}$$

Eqn. 5 describes the compensated sensor response as a function of the mirror distance. The response still depends on $R(d_{\mathrm{M}})$ as for the sensor without compensation (see Eqn. 1), but the presence of a real filter introduces a constant term $k \cdot a_0$ due to a small amount of the measurement signal (λ_2) that is partially reflected by the filter and that perturbs the signal reflected by the

mirror. At large distances, this unwanted signal becomes prevalent thus reducing the sensor range, as will be experimentally shown in the next section.

IV. Experimental results

A. The experimental setup

To test the effectiveness of the proposed compensation technique, a displacement sensor has been arranged as shown in Fig. 3.

A multi-color LED is employed to generate optical signals having three different wavelengths: 625 nm (red), 525 nm (green) and 465 nm (blue). Even though the red signal is not the best choice when standard POF are employed [13], this multi-color LED has the advantage of allowing removing the coupler of Fig. 2 and thus providing better stability, since it is well known that multimode POF couplers have typically poor directivity. The LED is driven at constant current and an electronic switch is employed to turn on/off the different optical sources. The optical signals are modulated sinusoidally at low frequency (about 1 kHz) to improve the noise rejection through a synchronous detection. Two step-index PMMA plastic optical fibers having about 1 mm core diameter are coupled to the LED and to the photodetector (PD), respectively. The PD output is amplified with a transimpedance amplifier and the signals are measured by a general purpose acquisition board and a synchronous detection algorithm. The fiber bundle is fixed on a manual precision translation stage and positioned in front of a 2 mm-thick dichroic filter (d_0), whose optical response is shown in Fig. 4. The figure also shows the LED spectra as measured before the tests using a high resolution CCD-based spectrometer. It is possible to see that the filter transmittance at 465 nm (blue light) is $T_2 \simeq 90\%$ and at 625 nm (red light) is $T_1 < 1\%$, whereas the green light is located at the filter transition band. Since the filter provides the best separation when used with the red and the blue LED emissions, these are the two wavelengths that have been employed in the sensor implementation.

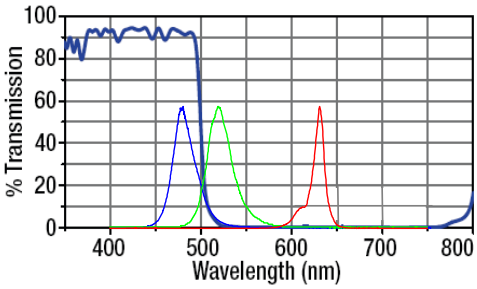

Fig. 4. The optical response of the dichroic filter (produced by Thorlabs) employed in the setup and the LED spectra.

A second linear stage is employed to move the mirror in order to characterize the sensor response to displacement. This stage embeds a motorized actuator that is controlled by means of a Personal Computer (PC). The PC sets the mirror distance d from the filter, acquires the detected signal and controls the switch used to select the LED emission wavelength. Fig. 5 shows the optical section of the experimental setup. The optical signals at the two filter sides are shown in Fig. 6: the transmitted blue light intensity is greater than the red one, as expected.

B. Effects of the filter position and sensor range

The filter position affects the amplitude of the compensation signal since this is almost completely reflected by the filter. In order to maximize the signal amplitude, and therefore minimize its uncertainty, the filter can be located at the optical peak that, in our setup, is at about 1 mm from the fiber tips. This choice also allows minimizing the sensitivity of the reference signal with the filter position, that may change because of thermal

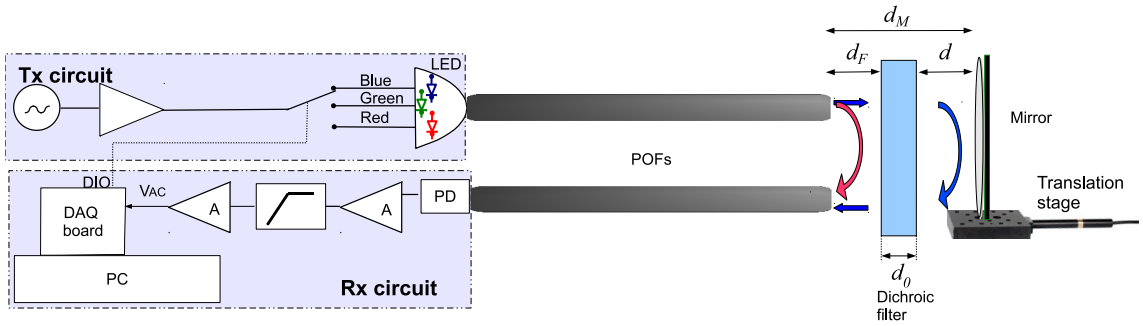

Fig. 3. The realized setup to test the effectiveness of the technique to compensate power fluctuations in displacement sensors.

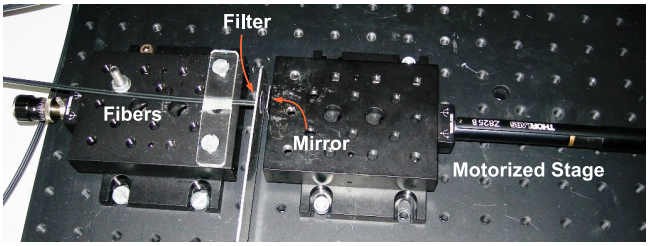

Fig. 5. Photograph of the optical part of the experimental setup.

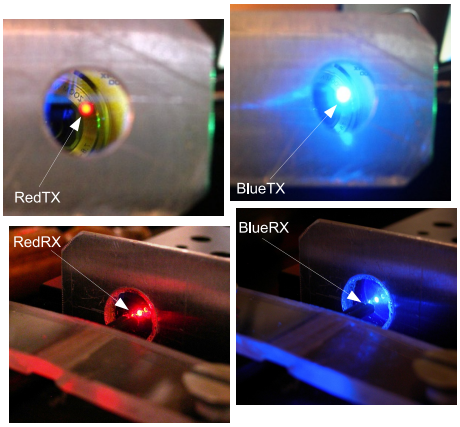

Fig. 6. Photograph of the optical red and blue signals: transmitted (top) and reflected (bottom).

and mechanical stability issues. However, in our setup, the filter has been positioned at a shorter distance (about 0.5 mm) in order to enlarge the mirror excursion and thus the sensor working range. Indeed, the lower end of the

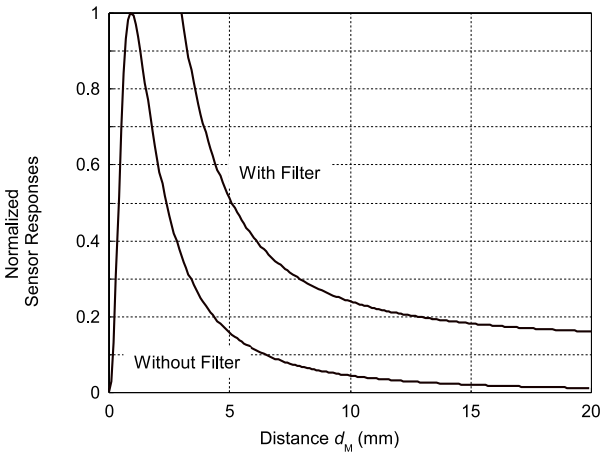

Fig. 7. Sensor optical response with and without compensation filter.

working range is determined by the filter position and thickness, whereas the upper end is limited by the conditioning circuit noise. As an example, in our setup, the sensor response computed using Eqn. 5 has the behavior shown in Fig. 7. The response is drawn from about 3 mm, taking into account the filter position d_F=0.5 mm, the d_0=2 mm filter thickness and about 0.5 mm of clearance between the filter and the mirror. The response, decreasing as expected, presents a non zero horizontal asymptote because of the offset in Eqn. 5. This offset limits the usable range because it increases the effect of noise on the measured distance by reducing the response

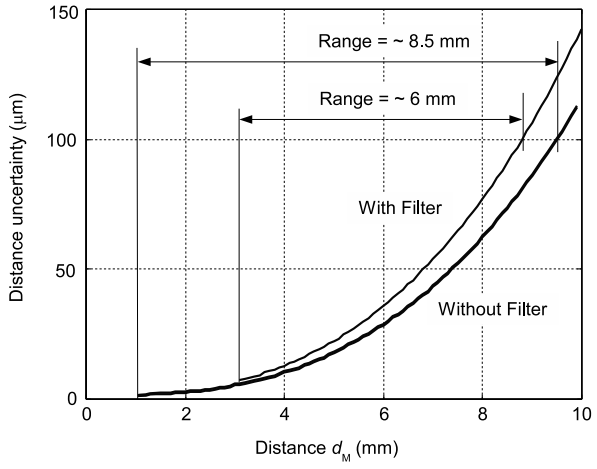

Fig. 8. Effect of the measurement noise on the distance standard uncertainty.

slope for increasing distance. As a comparison the figure shows the response of the same sensor without the filter (i.e. without compensation), evidencing the wider operating range of the uncompensated sensor because its response goes to zero asymptotically. Noise effects have been evaluated on the measured distance using the sensor optical models and estimating that the noise amplitude is about 0.1% of the detected signal range. The corresponding distance uncertainties are shown in Fig. 8 for the sensor with and without compensation. In both sensors the uncertainty increases with distance and the sensor with the filter exhibits a larger value. The figure also shows the sensor working ranges assuming that the maximum tolerable uncertainty is 100 μm. The sensor without compensation has an operating range that spans from about 1 mm (i.e. the received peak power position), up to about 9.5 mm, while the compensated sensor only from 3 mm to about 9 mm.

C. Tests at different optical power levels

Tests have been carried out in order to assess the effectiveness of the proposed compensation technique in the range (0 to 10) mm by changing the mirror to filter distance d in 50 μm steps.

At each step the red and blue lights have been turned on/off alternatively and the corresponding detected signals measured by means of the acquisition board. The distance d_{F} between the fiber tips and the filter has been kept constant so the red signal, which is almost completely reflected by the filter, has an almost constant amplitude and can be employed as the compensating signal. The blue signal, instead, is almost completely transmitted by the dichroic filter and so it is used to retrieve the distance d.

Three tests have been carried out at different optical power levels (namely test#1: 100%, test#2: 75% and test#3: 50% in Fig.s 9, 10, 11), emulating a severe change in fiber propagation loss affecting both signals. Fig. 9 reports the red signal amplitudes as measured during the tests; the signals are proportional to the optical power and are constant during each test, regardless of the mirror distance.

The blue signal amplitudes are shown in Fig. 10. The three signals are still proportional to the optical power, but they decrease with distance, since the sensors are working in the rightmost part of the characteristics.

The ratio between the blue and red signals is reported in Fig. 11: it can be observed that the curves overlap because the ratio depends on the distance and is not influenced by the launched power, thus confirming the compensation capability of the proposed technique.

The metrological performance has been investigated using test#1 (100% optical power) as a calibration curve and computing the displacement error that arises when the sensor is working at a reduced optical power. Fig. 12 shows, for each displacement, the displacement error whose behavior is in agreement with the result of Fig. 8. The error remains below 100 μm for displacements up

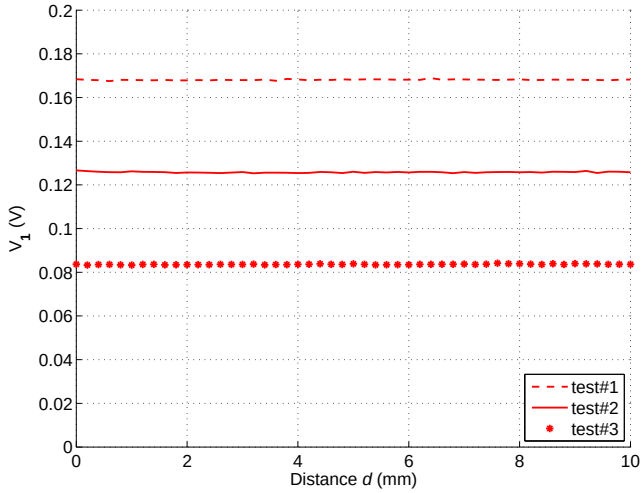

Fig. 9. Red signal amplitudes measured at three optical power levels (100%, 75%, 50%) for mirror distance in the range of (0 to 10) mm

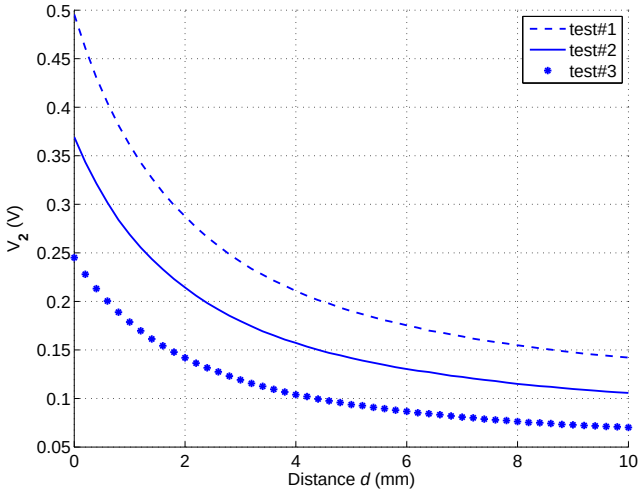

Fig. 10. Blue signal amplitudes measured at three optical power levels (100%, 75%, 50%) for mirror distance in the range of (0 to 10) mm.

to 6 mm. As a comparison, if the sensor is employed without any compensation (that is, only the blue signal is considered), the retrieved displacement would be in the range 0.3 mm to 4.3 mm in the case of detected signal of 0.2 V (see Fig. 10), yielding an error of about ± 2 mm. The maximum residual error of Fig. 12 is mainly due to the slightly wavelength-dependent response of the active optical components (LED and PD) to temperature as well as to the mechanical setup stability, since the test was performed over a period of several hours. At large displacements, the error is dominated by noise, while other effects, such as the stability of the fiber losses at different wavelengths, do not affect significantly the results.

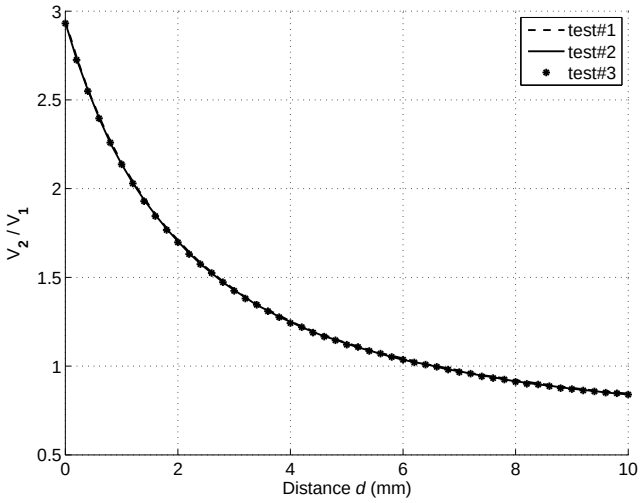

Fig. 11. The blue/red signal ratio at three optical power levels (100%, 75%, 50%) for mirror distance in the range of (0 to 10) mm.

D. Thermal tests

The previous test has proven the capability of the compensation technique to mitigate optical power changes. In practical cases, however, optical power instabilities are mainly due to fiber scattering loss and intrinsic attenuation, both strictly dependent on the fiber material composition [14] and on the environmental conditions. Some experimental results [15] have shown a significative wavelength dependence of the fiber attenuation because of the different phenomena that occur in polymeric materials, and such a behavior may corrupt the dual wavelength compensation since the red and blue signals could drift differently. For these reasons the choice of the

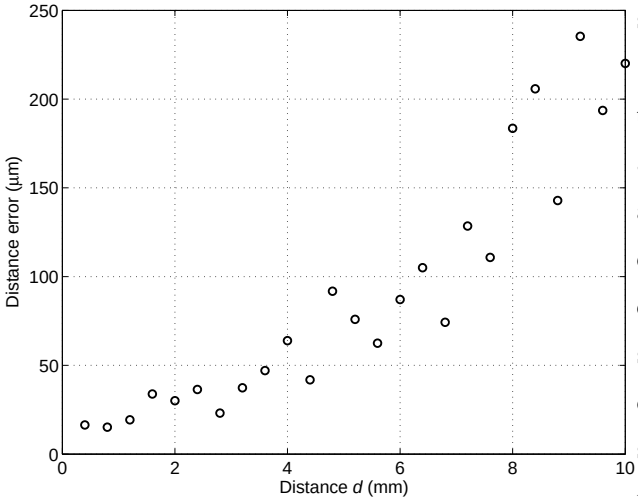

Fig. 12. Distance error evaluated at different power levels.

two wavelengths requires a further investigation on the fiber behavior. Choosing two wavelengths closely spaced would provide the best results but it is then difficult to be implemented at a reasonable cost since it requires very selective filters. On the contrary, the wavelengths employed in the previous test can be easily separated by a low-cost dichroic filter, but their spectral distance may be too large to provide a satisfactory compensation for some POF exposed to environmental condition changes. Therefore, tests have been performed with the available fibers and sources to find the fiber/sources combination that provides good compensation results without requiring expensive filters. Among the samples from different manufacturers, a 20 m span of multicore POF having 1 mm diameter has been selected since it has similar attenuation temperature changes at the red and green light. To this aim, the third junction of the LED, whose peak wavelength is at 525 nm, has been employed as the measurement signal, even though it is only partially transmitted by the available filter, while the red signal is still employed as the reference signal. The non ideal filter transmission coefficient at the green light affects the sensor sensitivity and further reduces the sensor range.

A climatic chamber has been employed to change the fiber temperature (T_{F} in Fig. 13(a)) from $8\,^{\circ}$C to $50\,^{\circ}$C while the sensor was maintained at a fixed position at ambient temperature (T_{S}, in the same figure). The detected signals have been recorded and their relative changes are shown in Fig. 13(b) where it is possible to see that the temperature affects both signal amplitudes of about $\pm$ 5%, corresponding to a fiber temperature sensitivity of about 0.25%/°C. Without compensation, i.e., considering the green signal only, the reported signal change corresponds to an apparent displacement of up to $\pm$1.7 mm since the sensor sensitivity, obtained experimentally, is of about -3%/ mm. The effect of the compensation is shown in Fig. 13(c) where the signal ratio is plotted. The temperature effect is still present but its effect on the distance measurement is now of about $\pm$0.3 mm only. The figure also shows that the implemented system is able to compensate the unwanted signal drift due to a poor sensor setup, as it can be seen comparing the red and green signals measured at the beginning and at the end of the test.

V. Conclusions

A compensation system based on a dual-wavelength approach to produce a couple of measurement and reference signals suitable to be used in a low-cost optical sensor for displacement measurements has been described and deeply analyzed. The sensor is made of plastic optical fibers faced to a mirror and employs an inexpensive interrogation system based on amplitude detection in which the reference and the measurement signals travel along the same fibers and experience the same power fluctuations due to aging and environmental perturbations.

An optical model of the compensated sensor that takes

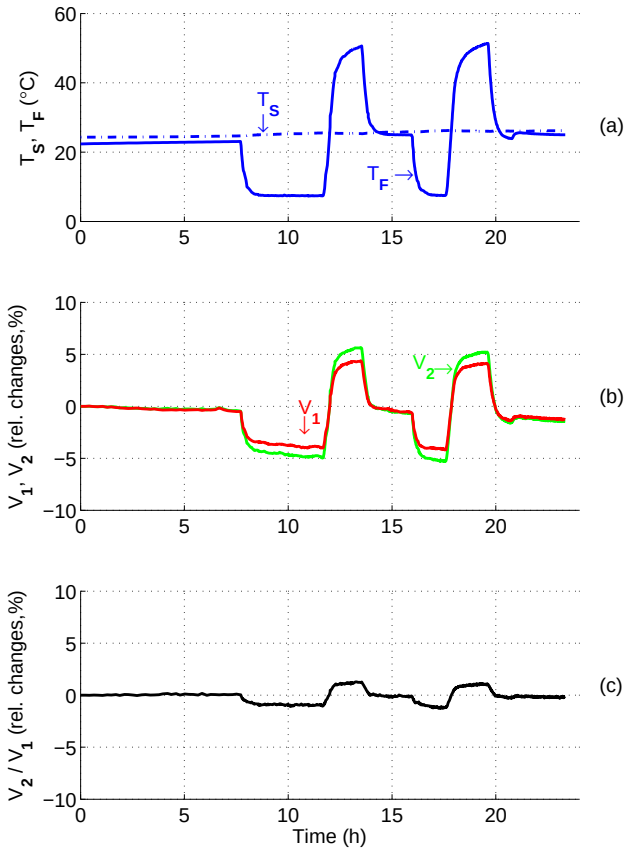

Fig. 13. Temperature test of a multicore fiber employed to arrange a compensated sensor. Fiber and sensor temperature (a), measurement and reference signals (b), signal ratio (c). The sensor sensitivity at the working distance is of about -3%/mm.

into account the filter effects has been developed and presented. According to the model results, the sensor is able to compensate optical power fluctuations that influence both wavelengths, although the presence of real filters reduces the sensor operating range.

Experimental tests have been carried out in a range up to 10 mm and at different optical powers. The results have shown that this arrangement can compensate power fluctuations up to 50% of the set value and still measure a displacement of 6 mm with a maximum error below 100 μm, error that is mainly due to the measurement noise, mechanical instabilities and source thermal effects.

Further tests have been performed at a fixed distance exposing the fiber at different temperatures in order to force a wavelength dependent attenuation change. These tests have shown that the attenuation drift in the polymers constituting the common types of plastic optical fibers depends significantly on the wavelength; as a consequence, an effective compensation can be obtained only using a proper wavelength combination for measurement and reference signals. Stability tests carried out using a multicore POF and green/red LED have shown a significative reduction of the sensor temperature effects from 0.25%/°C to 0.05%/°C.

Hence, it has been demonstrated that the proposed compensation technique can be successfully used either alone or to complement the dummy sensor technique previously developed, in order to enhance the long-term stability of sensor stability against environmental disturbances, such as temperature variation and mechanical stresses acting on the fibers. Indeed, multi year-long comparative tests, which are currently in progress in a prestigious monumental building using a sensor network deployed over quite a large area, are confirming the improvement in the long-term sensor stability after application of the proposed dual wavelength compensation approach.

REFERENCES

[1] F. Ansari, “Fiber optic sensors for structural health monitoring of civil infrastructure systems”, in *Structural Health Monitoring of Civil Infrastructure Systems*,Woodhead Publishing, 2009.

[2] M. Lequime, “Fiber sensors for industrial applications”, in *Optical Fiber Sensors*, OSA Technical Digest Series, paper OTuD1, 1997.

[3] B. Glisic, D. Inaudi, *Fibre optic methods for structural health monitoring*, John Wiley and Sons Ltd, 2007.

[4] D.C. Lee, J.J. Lee, I.B. Kwon, D.C. Seo, “Monitoring of fatigue damage of composites structures by using embedded intensity-based optical fiber sensors”, *Smart Mater. Struct*, vol. 10, pp. 285-292, 2001.

[5] G. Perrone, A. Vallan, “A low-cost optical sensor for non contact vibration measurements”, *IEEE Trans. Instrum. Meas.*, vol. 58, no. 7, pp. 1650-1656, 2009

[6] M. Olivero, G. Perrone, A. Vallan, S. Abrate, “Plastic optical fiber displacement sensor for cracks monitoring”, *Key Eng. Mater.*, vol. 347, pp. 487-492, 2007.

[7] D. S. Montero, C. Vzquez, I. Mllers, J. Arre , D. Jger, “A Self-Referencing Intensity Based Polymer Optical Fiber Sensor for Liquid Detection”, vol.9, *Sensors*, pp. 6446-6455, 2009.

[8] M.L. Casalicchio, A. Penna, G. Perrone, A. Vallan, “Optical fiber sensors for long- and short-term crack monitoring”, *Proc. of IEEE Workshop on Environmental, Energy, and Structural Monitoring Systems (EESMS 2009)*, Crema, Sept. 25th 2009, pp. 87-92, 2009.

[9] M.L. Casalicchio, M. Olivero, G. Perrone, A. Vallan, “Plastic Optical Fiber Sensor for Displacement Monitoring with Dual-Wavelength Compensation of Power Fluctuations”, *I2MTC 2011 - Proc. of IEEE Instr. and Meas. Tech. Conf.*, Hangzhou, May, 10-12th 2011, pp. 832-836, 2011.

[10] G. Murtaza, J. M. Senior, “Dual wavelength referencing of optical fibre sensors”, *Opt. Commun.* , vol. 120, pp. 348-357, 1995.

[11] G. Perrone, M. Olivero, A. Vallan, A. Carullo, A. Neri, “Long term in-situ test of a low-cost fiber-based crack monitoring system”, *Proc. of IEEE Sensors Conf. 2008*, Lecce, Oct, 26-29th 2008.

[12] M. L. Casalicchio, M. Olivero, A. Penna, G. Perrone, A. Vallan, “Distributed POF sensor network for crack monitoring in buildings”, *Proc. of POF’10*, Yokohama, Oct, 19-21 th , 2010.

[13] O. Ziemann, J. Krauser, P.E. Zamzow, W. Daum, “Fundamentals of optical fibers-attenuation”in *POF Handbook: Optical Short Range Transmission Systems*, *Springer*, 2nd Edition, p. 46-47, 2008.

[14] F. Chunyuan, R. Zhongyang, “Research on Measurement of POF Attenuation Spectrum”, *Proc. of IEEE Intelligent Computation Technology and Automation (ICICTA 2011)*, Shenzhen, Mar, 28-29th, 2011, vol. 2, pp. 672-674, 2011.

[15] A. Appajaiah, “Climatic Stability of Polymer Optical Fibers (POF)”, *BAM Dissertation Series*, available on line at http://www.bam.de/ , Vol. 9, 2005.

PLACE PHOTO HERE

Alberto Vallan received the M.S. degree in Electronic Engineering from Politecnico di Torino (Italy) in 1996 and the Ph.D. degree in Electronic Instrumentation from the University of Brescia (Italy) in 2000. He is currently an assistant professor at the Politecnico di Torino, Department of Electronics. His main research interests are in the field of sensors and instruments for industrial applications.

PLACE PHOTO HERE

Maria Luisa Casalicchio received the M.S. degree in Electronic Engineering in 2007 from Politecnico di Torino (Italy). She is currently a Ph.D. student in Metrology at the same University. Her main fields of interest are the development and the metrological characterization of acquisition systems and fiber optic sensors.

PLACE PHOTO HERE

Massimo Olivero Massimo Olivero received the M.Sc. in Electronic Engineering and the Ph.D. in Photonics from Politecnico di Torino, Italy, in 2002 and 2006 respectively. In 2004-2005 he worked as a Visiting Researcher at the Technical University of Denmark on the development of integrated optical devices by direct UV writing. From 2006 to 2008 he was post-doctoral researcher at Politecnico di Torino, conducting research on optical measurements and characterization of nanostructured materials. He is currently part of the Senior Engineer Staff at the Photonics Lab of Politecnico di Torino, where he works on fiber components for high power lasers and fiber optics sensors.

PLACE
PHOTO
HERE

Guido Perrone holds a Ph.D. in Electromagnetics from Politecnico di Torino (Italy), where he is currently professor at the Department of Electronics, lecturing on Optical Components and Fibers and on Microwave Devices. His research activity is mainly in the fields of fiber optical sensors and of high power fiber lasers. Dr. Perrone is member of IEEE/MTTS, of IEEE/Photonics Society and of the Optical Society of America.